

Air-Gaps for Electrical Interconnections

Paul A. Kohl,^{a,*} Qiang Zhao,^{a,c} Kaushal Patel,^a Douglas Schmidt,^{a,*}
Sue Ann Bidstrup-Allen,^a Robert Shick,^b and S. Jayaraman^b

^a School of Chemical Engineering, Georgia Institute of Technology, Atlanta, Georgia 30332-0100, USA

^b BFGoodrich Company, Brecksville, Ohio 44141, USA

^c Present address: AlliedSignal, Sunnyvale, California 94089, USA

The fabrication of air-gap structures for electrical interconnections has been demonstrated using a sacrificial polymer encapsulated in conventional dielectric materials. The air-gap is formed by thermally decomposing the sacrificial polymer and allowing the by-products to diffuse through the encapsulating dielectric. The diffusivity of the polymer decomposition products is adequate at elevated temperatures to allow the formation of an air-gap. The decomposition of a 5 μm thick polymer film results in less than 100 \AA of residue. Electromagnetic simulation shows that the effective dielectric constant of silicon dioxide ($\epsilon = 4.2$) can be lowered to 2.4-2.8 for relevant structures.

© 1998 The Electrochemical Society, Inc. S1099-0062(98)01-087-6

Manuscript received January 30, 1998.

The National Technology Roadmap for Semiconductors calls for the qualification/preproduction of low dielectric constant (low- k) insulators for integrated circuit (IC) interconnections in the 1999 ($k = 2.5$ -3.0) to 2006 ($k = 1.5$) timeframe.¹ The need for low- k materials originates from the shrinkage in transistor area creating signal propagation delays, crosstalk noise, power dissipation due to resistance-capacitance (RC) coupling, and an increase in the number of interconnection levels. The problem is most severe for global interconnects.² At sub-0.5 μm technologies, the intralevel capacitance is the major contributor to the RC delay.³

A number of materials are being investigated to replace SiO_2 used for ICs ($k \sim 4.2$). Initiatives to introduce low- k materials for interconnections at other levels of packaging are also underway. The low- k materials options include: inorganic siloxane-based polymers (O-Si-O backbone),^{4,5} polyimides,⁶ benzocyclobutenes,^{6,7} polyarylene ethers,^{8,9} hydrogen- and organosilsesquioxanes,^{10,11} parylene and parylene copolymers,^{12,13} and polynorbornene.¹⁴

The incorporation of air (or other gases) into the dielectric material is a promising approach to achieving ultralow- k insulators. Nanoporous silica films have attracted interest because the material is similar (i.e., precursors used in deposition, chemical processing, and physical properties) to the silica films currently used.¹⁵ Thus, low- k performance can be achieved while retaining some of the silica-based properties and infrastructure.

In this paper, we demonstrate an air-gap concept based on a sacrificial polymer and plasma-enhanced chemical vapor deposited (PECVD) SiO_2 (or other dielectrics). Functionalized polynorbornene was used as the sacrificial polymer. There are several objectives of this air-gap process. First, the air-gap is formed between adjacent metal lines (in-plane) reducing the intralevel dielectric constant. The intralevel capacitance has been shown to be the major contributor to the RC delay for sub-0.5 μm interconnections, as opposed to the interlevel capacitance being the major contributor for larger-size technologies.³ Second, the dielectric material on top of, and below the metal/air-gap structure (the interlevel dielectric material), should be an established insulator used in IC or packaging applications. The use of porous materials, such as foams or xerogels have advantages in forming air-gaps (e.g., high diffusivity for gases), or can themselves be thought of as partial air-gaps, however, wide scale availability and use has not taken place. Third, the air-gap will be formed after a contiguous film of interlevel dielectric material (overcoat dielectric) has been deposited and processed (i.e., cured in the case of polymer dielectrics). The processing conditions during formation of the air-gap should be compatible with the interlayer (overcoat) dielectric. For example, a high-temperature oxygen atmos-

phere is not acceptable for many organic dielectrics. Fourth, the creation of the air-gap should not deposit or create undesirable residues in the intralevel region between the metal lines. Anand et al. have shown that sputtered carbon can be used as a sacrificial material in the formation of air-gaps, however, a high-temperature oxidation of the carbon with O_2 is required making it incompatible with some dielectrics.¹⁶ It is shown that the sag in the overcoat dielectric is minimal during processing. In a similar process, Havemann and Jeng have used the oxidation of photoresist and other organic materials to form gas cavities for interconnections.¹⁷ In these studies, the residue or char resulting from the oxidation of the organic material was not quantified.

The air-gap process sequence using a sacrificial, thermally decomposed polymer is shown schematically in Fig. 1. A planar metal-polymer structure is shown in Fig. 1a. The intralevel (sacrificial) polymer will be thermally decomposed forming an air-gap in a later process step. The metal-polymer structure in Fig. 1a can be

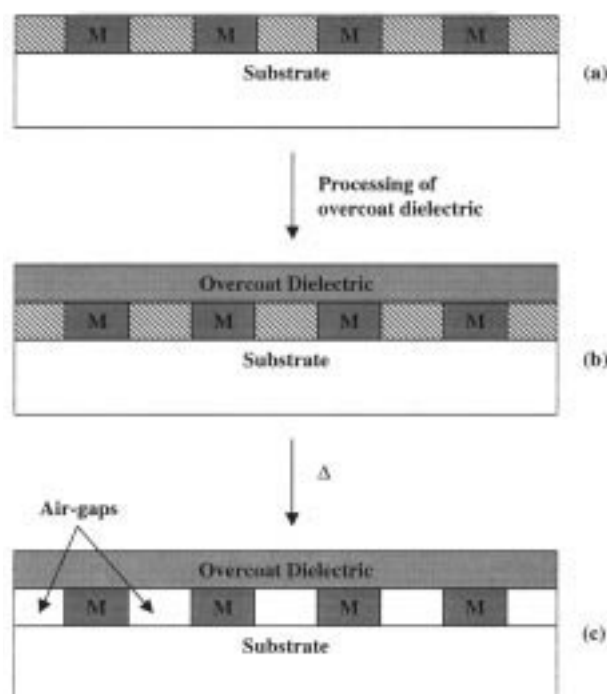


Figure 1. Diagram of air-gap structure. (a) The sacrificial layer is formed between metal lines (M). (b) An overcoat dielectric layer is deposited over the metal/sacrificial polymer layer. (c) The air-gap is formed by decomposing the sacrificial polymer.

* Electrochemical Society Active Member.

† E-mail: paul.kohl@che.gatech.edu

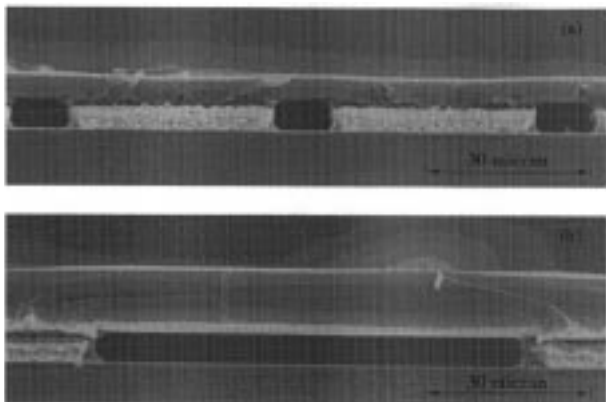


Figure 2. Cross-sectional view of air-gap formed between metal lines with overcoat dielectric.

formed in a variety of ways. The polymer can be deposited first by spin-coating, spraying, or other methods followed by patterning. Reactive ion etching (RIE), laser ablation, wet chemical etching, or photosensitivity can be used to pattern the sacrificial polymer. Once the polymer has been patterned, the metal can be in-laid between the polymer regions in a Damascene-type process using blanket metal deposition (via physical vapor deposition, chemical vapor deposition, or electroplating) followed by chemical mechanical polishing (CMP). An alternate method of fabricating the structure in Fig. 1a is to first pattern the metal by additive, semi-additive, or subtractive means, followed by a Damascene process for the polymer using blanket-coating followed by CMP. Alternately, the blanket layer of polymer over the metal electrodes could be etched back using RIE. Once the metal-polymer structure is in place, as shown in Fig. 1a, an overcoat or interlevel dielectric material can be deposited and processed (e.g., cured) as shown in Fig. 1b. The intralevel polymer must be able to withstand the processing conditions used to process the interlevel dielectric. Once the interlevel dielectric is in place, the structure is heat-treated in an inert atmosphere causing the decomposition of the sacrificial, intralevel polymer creating the air-gap, as shown in Fig. 1c. While the gas remaining in the voids in Fig. 1c is not air during the decomposition process, it is assumed that gaseous exchange with air will take place over a period of time.

A cross section of a fabricated metal/air-gap structure is shown in Fig. 2. In this demonstration, 5 μm of functionalized polynorbornene (PNB, Unity 400™ Polymer, BFGoodrich, Brecksville, OH) was deposited by spin-coating onto a Ti/Au ground plane. 20% of the norbornene monomers were functionalized with a triethoxysilyl group, which provided adhesion and possibly a controlled rate of decomposition. The Ti layer (100 Å thick) provided adhesion between the lower dielectric layer [Si(100) with a thick thermal oxide] and the Au (1000 Å thick). The PNB was patterned by RIE using a silicon dioxide mask with the pattern transferred from a photoresist layer.¹⁸ The gold metal was electroplated using the PNB as the plating mold. Similar structures were prepared using a seed layer of Cr/Cu with electroplated Cu lines. Although the metal lines are electrically interconnected through the ground plane, the demonstrations serve as structural test vehicles. The interlayer dielectric (overcoat dielectric) was 5 μm of PECVD silicon dioxide deposited at 200°C, OCG Prohimide 412 or Amoco Ultradel 7501 polyimide. Figure 2a shows 10 μm wide and 5 μm high air-gaps. Figure 2b shows a wider air-gap (ca. 80 μm), with the same 5 μm height. The metal/air-gap structures were several centimeters long and fully encapsulated with the overcoat dielectric. The air-gaps were formed by thermally decomposing the PNB at 425-450°C for 1 h using a slow ramp rate on the heating cycle in a nitrogen atmosphere. A typical cycle was heating 5°C/min to 375°C with a 5 min hold at 375°C, heating at 1°C/min to 400°C with a 5 min hold at 400°C, followed by heating at 1°C/min to the final temperature in a nitrogen atmos-

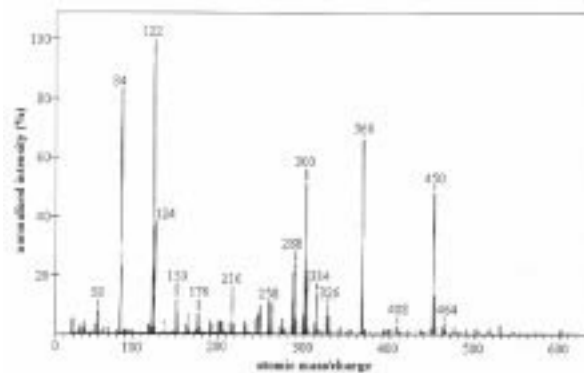


Figure 3. Mass spectrum of decomposition products of functionalized PNB.

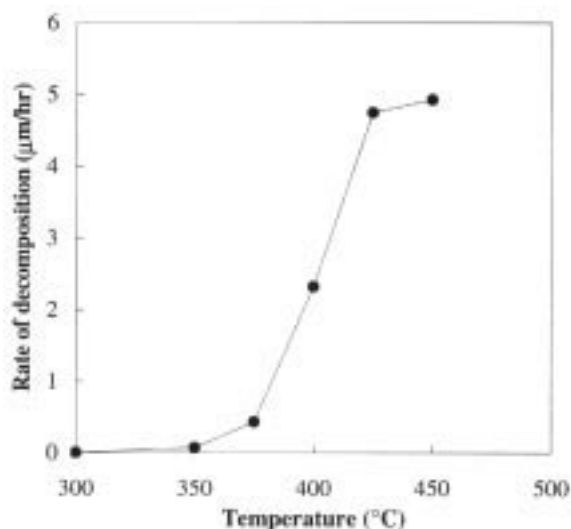


Figure 4. Decomposition rate of functionalized PNB as a function of temperature.

phere. The thickness of the overcoat dielectric is greater than that needed for ICs, however, it shows the ability to permit the diffusion of the decomposition products at the reaction temperature. The width of the air-gaps confirms the modeling results of Anand et al. which indicated that the overcoat dielectric would not sag.¹⁶

During formation of the air-gap, the encapsulated PNB thermally decomposes and the gaseous decomposition products diffuse through the overcoat dielectric layer. The mass spectrum of the decomposition products of freestanding (not encapsulated) films of PNB was measured. Figure 3 shows a mass spectrum for PNB at 300-360°C. The data was collected during a temperature ramp from 300 to 360°C. The major peak at 450 mass/charge ratio (m/q) corresponds to norbornene trimers. The triethoxysilyl group appears to form volatile units with PNB: silanized norbornene dimers (556 m/q), silanized PNB trimers (706 m/q), and silanized PNB with cyclopentadiene complex (472 m/q). Mass analysis of the PNB products at different temperatures or when encapsulated by an overcoat dielectric were not measured due to the complexity of the experiments. The rate of decomposition of the PNB was critical to the structural integrity of the air-gaps. The average rate of PNB decomposition vs. temperature is shown in Fig. 4. The data points were obtained by measuring the thickness of PNB films before and after a 1 h temperature soak in a nitrogen-purged chamber. Excessively high decomposition rates resulted in the rupture of the overcoat material due to pressure buildup within the air-gap cavity.

Table I. Atomic percent of PNB residue measured by XPS for decompositions performed at different temperatures.

Temperature, °C	Carbon	Oxygen	Silicon
300	92.7	4.0	3.3
400	92.1	4.2	3.7
425	89.4	5.8	4.8
450	83.5	7.9	8.7
500	80.3	10.4	9.4

Optical examination of the surface of thermally decomposed PNB showed especially clean, and residue-free surfaces. X-ray photoelectron spectroscopy (XPS) was used to analyze the substrate surface after PNB decomposition. The composition and thickness of the residue was estimated using standard sensitivity factors and argon ion sputtering, respectively. The experiments were performed on a gold surface because gold was not an impurity in the PNB and served as a convenient end point for the XPS thickness analysis. A thin residue was found on the surface and was composed primarily of C, O, and Si. The thickness of the residue was estimated by Ar ion sputtering. The Ar ion etch rate was calibrated by etching thermally grown SiO₂. Based on the etch rate of SiO₂, the PNB residue was approximately 100 Å thick. Elemental analysis of the surface after decomposition of 5 μm of PNB at different temperatures is shown in Table I. The silicon content of the residue originates from the triethoxysilyl group attached to the polynorborene. The oxygen content appears to be a reaction product with residual oxygen in the nitrogen furnace or ethoxy residue from the triethoxysilyl groups. The C:O:Si atomic ratio becomes more silicon rich at higher temperature reaching a value of about 10:1:1 for decomposition at 450°C. The presence of trace impurities in the PNB on the quantity of residue was not determined.

The effective in-plane dielectric constant (ϵ_{eff}) of an air-gap encapsulated between two parallel metal lines was simulated using an electrostatic simulator (Maxwell Corp.). The geometry of the simulated structure is shown in Fig. 5. The values of ϵ_{eff} are presented as a function of height of the air-gap and thickness of the encapsulating (overcoat) dielectric above and below the metal/air-gap structure (equal lines and spaces), as a function of the dielectric constant of the overcoat dielectric. For example, the ϵ_{eff} of silicon dioxide ($\epsilon = 4.0$) can be lowered to 2.3-2.7 by fabricating an air-gap between the metal lines for structures with 1:1 aspect ratio (as high as they are wide), depending upon the thickness of the dielectric layer. If the height of the metal lines is twice the width of the lines and spaces, the ϵ_{eff} would be about 1.8 to 2.2, depending on the height of the dielectric above the metal lines. It would be very difficult to drop ϵ_{eff} below 2.0 using fully densified silicon dioxide and an air-gap. One could drop ϵ_{eff} below 2.0 with a modest drop in the dielectric constant of the overcoat material (e.g., 3.5) with an air-gap.

In summary, the ability to fabricate air-gaps in electrical interconnections has been demonstrated by use of a sacrificial polymer embedded between metal interconnection structures and fully encapsulated by an overcoat dielectric. The sacrificial polymer is thermally decomposed at a controlled rate. At the decomposition temperature, the products diffuse through the overcoat dielectric leaving an air-gap with very little residue. Air-gap structures can lower the

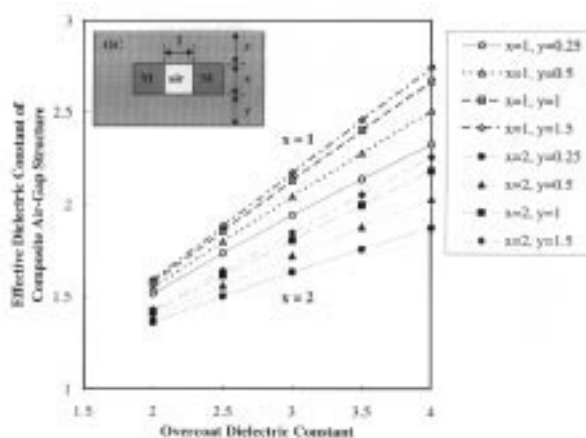


Figure 5. Effective dielectric constant of a metal/air-gap structure for a variety of dimensions.

intralevel dielectric constant of silicon ($\epsilon = 4.0$) to ca. 2.5 for structures with equal lines and spaces. Thus, the infrastructure built around SiO₂ can be used for producing low-k interconnections.

The Georgia Institute of Technology assisted in meeting the publication costs of this article.

References

1. *The National Technology Roadmap for Semiconductors*, Semiconductor Industry Association, San Jose, CA (1997).
2. J. D. Meindl, *Proc. IEEE*, **83**, 619 (1995).
3. S.-P. Jeng, R. Havemann, and M. Chang, in *Advanced Metallization for Devices and Circuits - Science, Technology, and Manufacturing*, S. P. Murarka, A. Katz, K. N. Tu, and K. Maex, Editors, Vol. 337, p. 25, MRS, Pittsburgh, PA (1994).
4. H. Maruyama, N. Ohashi, M. Yoshida, Y. Taguma, N. Konishi, K. Kikishima, and N. Owada, in *Proceedings of the 14th International VLSI Multilevel Interconnection Conference*, p. 629 (1997).
5. S. Fukuyama, Y. Nakata, and M. Kobayashi, in *Proceedings of the 1st International Dielectrics for VLSI/ULSIMultilevel Interconnection Conference*, p. 80 (1995).
6. G. Messner, I. Turlik, J. W. Balde, and P. E. Garrou, *Multichip Modules*, ISHM, Reston, VA (1992).
7. S. Martin, M. Mills, P. Townsend, and D. Castillo, *Advanced Metallization and Interconnect Systems for ULSI Applications in 1995*, R. Ellwanger and S.-Q. Wang, Editors, MRS, Pittsburgh, PA (1995).
8. K. Lau, E. Brouk, T. Chen, B. Korolev, P. Schilling, and H. Thompson, in *Proceedings of the 14th International VLSI Multilevel Interconnection Conference*, p. 577 (1997).
9. R. Vrtis, K. Heap, W. Burgoyne, and L. Roberson, in *Low Dielectric Constant Materials and Interconnects Workshop Proceedings*, p. 221, SEMATECH (1996).
10. R. Leung, T. Nakano, S. Case, B. Sung, J. Yang, and D. Choi, in *Proceedings of the 3rd International Dielectrics for VLSI/ULSIMultilevel Interconnection Conference*, p. 49 (1997).
11. T. Nakano, K. Tokunaga, and T. Ohta, *J. Electrochem. Soc.*, **142**, 1303 (1995).
12. M. J. Szwarc, *Discuss. Faraday Soc.*, **2**, 46 (1957).
13. K. J. Taylor, M. Eissa, J. Gaynor, and H. Nguyen, in *Low-Dielectric Constant Materials III*, C. Case, P. A. Kohl, T. Kikkawa, and W. W. Lee, Editors, Vol. 476, MRS, Pittsburgh, PA (1997).
14. R. Shick, B. Goodall, L. McIntosh, S. Jayaraman, P. Kohl, S. Bidstrup-Allen, and N. Grove, in *Low Dielectric Constant Materials and Interconnects Workshop Proceedings*, p. 114, SEMATECH (1996).
15. C. Jin, J. D. Luttmer, D. M. Smith, and T. A. Ramos, *MRS Bull.*, **22**(10), 39 (1997).
16. M. B. Anand, M. Yamada, and H. Shibata, *IEEE Trans. Electron. Devices*, **44**, 1965 (1997).
17. R. H. Havemann and S.-P. Jeng, U.S. Pat 5,461,003 (1995).
18. Q. Zhao and P. A. Kohl, *J. Electrochem. Soc.*, **145**, 1257 (1998).